

Research Article

A Study of a Flow Model in Dual Permeability Reservoir Based on Similar Structure Theory

Tianhong Zhou ¹, Jie Shen ¹, Man Wang,¹ and Yun Wu²

¹School of Information Engineering, Wuhan Business University, Wuhan 430056, China

²School of Information Technology Application Innovation, Wuhan Polytechnic, Wuhan 436000, China

Correspondence should be addressed to Jie Shen; 20150623@wbu.edu.cn

Received 22 July 2022; Accepted 16 August 2022; Published 5 October 2022

Academic Editor: Junpeng Zou

Copyright © 2022 Tianhong Zhou et al. This is an open access article distributed under the Creative Commons Attribution License, which permits unrestricted use, distribution, and reproduction in any medium, provided the original work is properly cited.

The aim of the study is to further understand the rule of conversion of bottom hole pressure of a vertical well in a dual-permeability reservoir, which is about the dual permeability under different outer boundary (infinite, close, and constant value) conditions. However, there are few articles dealing with the model of a vertical well in a dual permeability reservoir under these three different outer boundary conditions. Hence, the paper proposes a model of a vertical well in a dual permeability reservoir under three outer boundary conditions. The model is solved with a Laplace space equation. We find the solution to the model that has a similar structure under three different outer boundary conditions by combining it with the similar structure theory. Therefore, we put forward a similar constructing method (SCM) that solves our model. The concrete steps of the SCM are given in this paper. At the same time, we draw the curves of the bottom hole pressure and pressure derivative using the modified Stehfest inversion formula and MATLAB software. In addition, we investigate the evolution of the pressure by changing the parameters (mobility ratio K , storability ratio ω , and crossflow coefficient λ). The solution to such a reservoir model obtained in this paper could be used as a basis for analyzing other typical reservoirs with vertical wells.

1. Introduction

The dual media is one of the largest storage formations in the world, and it is mainly composed of fracture and matrix media. Fluid flow in dual media can be treated in two kinds of models. One is the dual-porosity media model (Figure 1(a)), and the other one is the dual permeability media model (Figure 1(b)). In dual-porosity media, the fluid is stored in the matrix and flows into a wellbore through fractures, with a cross-flow from the fractures to the matrix, while in the dual permeability media model, the fluid flows into the wellbore not only from the fracture media but also from the matrix media, with a cross-flow between these two systems. Hence, the dual permeability is much more complicated than the dual-porosity media model. If we let the permeability of the dual permeability media model be equal to zero, then the dual permeability media model becomes the dual-

porosity media model. Thus, the dual-porosity media model can be considered as a special case for the dual permeability media model.

The study on dual permeability is mainly based on dual porosity and dual permeability. As regards the dual porosity model for horizontal wells, in 1988, Rosa and Carvalho [1] calculated the dynamic downhole pressure of horizontal wells in dual-porosity media by using the Stehfest Laplace transformation of the horizontal wells, which are widely used in the development of oil and gas reservoirs [2–8] with the progress in drilling and completion technologies. In 1994, a solution to the transient fluid flow of horizontal wells in a fractured dual porosity reservoir in Laplace space was obtained by Liu and Wang [9]. In 2012, Guo et al. studied the dual permeability flow behavior for modeling horizontal well production in fractured vuggy carbonate reservoirs [10].

In regards to the dual permeability model, in 1985, the solution to the vertical model under the outer

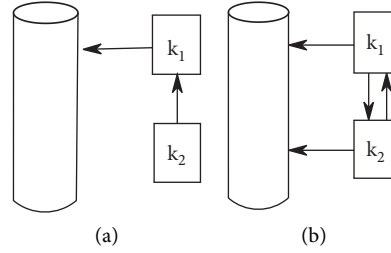


FIGURE 1: The sketch of the dual media. (a) Dual-porosity media; (b) dual permeability.

boundary infinite was first obtained through the Laplace transformation by Bourder [11]. In 1995, Liu and Wang [9] obtained the solution of the transient flow of slightly compressible fluid in the 2-D space, which provided a theoretical basis for related well test analyses. In 2006, the transient pressure in the dual permeability media of a shear-sensitive reservoir was studied by Tian and Tong [12]. In 2006, Hi and Tong [13] analyzed the effect of wellbore storage on bottom hole pressure in deformable dual permeability media by setting a mathematical model. In 2008, Liu [14] analyzed all kinds of reservoirs through the model curves under infinite boundary conditions in his literature. In 2010, Kong [15] obtained the solution of the vertical well in the dual permeability reservoir of signal and double layers by using Laplace and Weber's transformation and drew out the well test curve.

However, all the above studies are mainly based on the infinite outer boundary conditions, ignoring the close and constant outer boundary conditions. In 2004, the solution of a similar structure to the differential equation as a boundary value problem was put forward [16]. The influence of joints on the permeability and mechanical properties of rocks has been studied in some literature [17–19]. There were a lot of studies [20–26] about the vertical dual permeability reservoir under three different outer boundary conditions (infinite, close, and constant value). However, the studies in the references just stay at the math level, which cannot meet the demand of the well test analysis. Therefore, on the basis of the previous study, we set a model of a vertical well in the dual permeability reservoir under three outer boundary conditions (infinite, close, constant value) and solved the model in Laplace space. We found that the solution to the model has a similar structure under three different outer boundary conditions by combining with the similar structure theory. Hence, we put forward the SCM, and the concrete steps of the SCM are given in this paper. At the same time, we drew the curves of the bottom hole pressure and pressure derivative by using the modified Stehfest inversion formula and MATLAB software. We observed and analyzed the change law of the curves by changing the mobility ratio K , storativity ratio ω , and cross-flow coefficient λ . The solution to such a reservoir model obtained in this paper includes and improves the previous results and may then be used as a basis for analyzing other typical reservoirs with vertical wells.

2. Dimensionless Mathematics Model

The well is regarded as a point source in the paper, and supposing the outer boundary is a circular boundary. Therefore, according to [15], we can obtain the dimensionless mathematics model of the dual permeability reservoir as follows:

The seepage differential equation is as follows:

$$K \frac{1}{r_D} \frac{\partial}{\partial r_D} \left(r_D \frac{\partial P_{1D}}{\partial r_D} \right) + \lambda (P_{2D} - P_{1D}) = \omega \frac{\partial P_{1D}}{\partial t_D},$$

$$1 < r_D < R_D, t_D > 0, \quad (1)$$

$$(1 - K) \left(r_D \frac{\partial P_{2D}}{\partial r} \right) - \lambda (P_{2D} - P_{1D}) = (1 - \omega) \frac{\partial P_{2D}}{\partial t_D},$$

$$1 < r_D < R_D, t_D > 0,$$

where P is the reservoir pressure, MPa ; t is the time, h ; r represents any point in the reservoir at the radial distance of the well, m ; R is the outer boundary radius, m ; k is the permeability, μm^2 ; ω is storability ratio, dimensionless; λ is the cross-flow coefficient, dimensionless.

Initial condition is as follows:

$$P_{1D}(r_D, 0) = P_{2D}(r_D, 0) = 0. \quad (2)$$

Inner boundary condition is as follows:

$$\begin{cases} P_{wD}(t_D) = \left[P_{1D} - S_1 r_D \frac{\partial P_{1D}}{\partial r_D} \right]_{r_D=1} = \left[P_{2D} - S_2 r_D \frac{\partial P_{2D}}{\partial r_D} \right]_{r_D=1}, \\ \left[K r_D \frac{\partial P_{1D}}{\partial r_D} + (1 - K) \frac{\partial P_{2D}}{\partial r_D} \right]_{r_D=1} = - \left(1 - C_D \frac{\partial P_{2D}}{\partial t_D} \right), \end{cases} \quad (3)$$

where p_w is the bottom hole pressure, MPa ; S is the skin effect, dimensionless; C is the well storage, m^3/MPa .

Outer boundary condition is as follows:

$$P_{1D}(\infty, t_D) = P_{2D}(\infty, t_D) = 0,$$

$$\text{or } P_{1D}(R_D, t_D) = P_{2D}(R_D, t_D) = 0, \quad (4)$$

$$\text{or } \left. \frac{\partial P_{1D}}{\partial r_D} \right|_{r_D=R_D} = \left. \frac{\partial P_{2D}}{\partial r_D} \right|_{r_D=R_D} = 0,$$

where

$$\begin{aligned}
 P_{jD} &= \frac{1}{1.842 \times 10^{-3} Bq} \left(\frac{k_1 h_1}{\mu_1} + \frac{k_2 h_2}{\mu_2} \right) \\
 &\cdot [p_0 - p_j(r, t)] \quad (j = 1, 2), \\
 t_D &= \frac{3.6(k_1 h_1 / \mu_1 + k_2 h_2 / \mu_2) t}{(\phi_1 C_{t_1} h_1 + \phi_2 C_{t_2} h_2) r_w^2}, \\
 r_D &= \frac{r}{r_w}, \\
 C_D &= \frac{0.1592C}{(\phi_1 C_{t_1} h_1 + \phi_2 C_{t_2} h_2) r_w^2}, \\
 \lambda &= \alpha r_w^2 \frac{k_2 h_2 / \mu_2}{(k_1 h_1 / \mu_1 + k_2 h_2 / \mu_2)}, \\
 \omega &= \frac{\phi_1 C_{t_1} h_1}{\phi_1 C_{t_1} h_1 + \phi_2 C_{t_2} h_2}, \\
 K &= \frac{k_1 h_1 / \mu_1}{k_1 h_1 / \mu_1 + k_2 h_2 / \mu_2},
 \end{aligned} \tag{5}$$

h is the storage thickness, m ; μ is the viscosity, $mPa \cdot s$; r_w is the wellbore radius, m ; B is the oil volume coefficient, dimensionless; ϕ is the porosity, dimensionless; α is the shape factor, dimensionless.

3. Solutions in the Laplace Space

If we take the Laplace transformation of t_D of Eqs.(4)–(12), we obtain the following equation:

$$\begin{aligned}
 \bar{P}_{jD}(r_D, z) &= \int_0^\infty e^{-zt_D} P_{jD}(r_D, t_D) dt_D, \quad (j = 1, 2), \\
 \bar{P}_{wD}(z) &= \int_0^\infty e^{-zt_D} P_{wD}(t_D) dt_D,
 \end{aligned} \tag{6}$$

where z is the Laplace variable and $\bar{P}_{1D}, \bar{P}_{2D}, \bar{P}_{wD}$ are elements of Laplace space. Then, the form of the model in Laplace space can be obtained as follows:

$$\left\{ \begin{aligned}
 &K \frac{1}{r_D} \frac{d}{dr_D} \left(r_D \frac{d\bar{P}_{1D}}{dr_D} \right) + \lambda (\bar{P}_{2D} - \bar{P}_{1D}) = \omega z \bar{P}_{1D}, \\
 &(1 - K) \frac{1}{r_D} \frac{d}{dr_D} \left(r_D \frac{d\bar{P}_{2D}}{dr_D} \right) - \lambda (\bar{P}_{2D} - \bar{P}_{1D}) = (1 - \omega) z \bar{P}_{2D}, \\
 &\left[\bar{P}_{1D} - S_1 r_D \frac{d\bar{P}_{1D}}{dr_D} \right]_{r_D=1} = \left[\bar{P}_{2D} - S_2 r_D \frac{d\bar{P}_{2D}}{dr_D} \right]_{r_D=1} = \bar{P}_{wD}(z), \\
 &\left[K r_D \frac{d\bar{P}_1}{dr_D} + (1 - K) r_D \frac{d\bar{P}_2}{dr_D} \right]_{r_D=1} = - \left[\frac{1}{z} - C_D z \bar{P}_{wD} \right], \\
 &\bar{P}_{1D}(\infty, z) = \bar{P}_{2D}(\infty, z) = 0, \\
 &\text{or } \left. \frac{d\bar{P}_{1D}}{dr_D} \right|_{r_D=R_D} = \left. \frac{d\bar{P}_{2D}}{dr_D} \right|_{r_D=R_D} = 0, \\
 &\text{or } \bar{P}_{1D}(R_D, z) = \bar{P}_{2D}(R_D, z) = 0.
 \end{aligned} \right. \tag{7}$$

Theorem 1. If boundary value problem (7) has a unique solution, then the solution can be expressed as follows:

$$\begin{aligned} \bar{P}_{1D}(r_D, z) = & \frac{1}{z} \frac{C_D z + K a_2 + 1 - K / (1 - a_2) \Psi(1, \sigma_2) + S_2 - a_2 S_1 - K a_1 + 1 - K / (1 - a_1) \Psi(1, \sigma_1) + S_2 - a_1 S_1 / S_2 + \Psi(1, \sigma_2) / (1 - a_2) \Psi(1, \sigma_2) + S_2 - a_2 S_1 - S_2 + \Psi(1, \sigma_1) / (1 - a_1) \Psi(1, \sigma_1) + S_2 - a_1 S_1}{a_2 \Psi(r_D, \sigma_2) / (1 - a_2) \Psi(1, \sigma_2) + S_2 - a_2 S_1 - a_1 \Psi(r_D, \sigma_1) / (1 - a_1) \Psi(1, \sigma_1) + S_2 - a_1 S_1} \\ & \frac{S_2 + \Psi(1, \sigma_2) / (1 - a_2) \Psi(1, \sigma_2) + S_2 - a_2 S_1 - S_2 + \Psi(1, \sigma_1) / (1 - a_1) \Psi(1, \sigma_1) + S_2 - a_1 S_1}{\Psi(r_D, \sigma_2) / (1 - a_2) \Psi(1, \sigma_2) + S_2 - a_2 S_1 - (\Psi(r_D, \sigma_1) / (1 - a_1) \Psi(1, \sigma_1) + S_2 - a_1 S_1)} \\ \bar{P}_{2D}(r_D, z) = & \frac{1}{z} \frac{C_D z + K a_2 + 1 - K / (1 - a_2) \Psi(1, \sigma_2) + S_2 - a_2 S_1 - K a_1 + 1 - K / (1 - a_1) \Psi(1, \sigma_1) + S_2 - a_1 S_1 / S_2 + \Psi(1, \sigma_2) / (1 - a_2) \Psi(1, \sigma_2) + S_2 - a_2 S_1 - S_2 + \Psi(1, \sigma_1) / (1 - a_1) \Psi(1, \sigma_1) + S_2 - a_1 S_1}{\Psi(r_D, \sigma_2) / (1 - a_2) \Psi(1, \sigma_2) + S_2 - a_2 S_1 - (\Psi(r_D, \sigma_1) / (1 - a_1) \Psi(1, \sigma_1) + S_2 - a_1 S_1)} \\ & \frac{(\Psi(r_D, \sigma_2) / (1 - a_2) \Psi(1, \sigma_2) + S_2 - a_2 S_1) - (\Psi(r_D, \sigma_1) / (1 - a_1) \Psi(1, \sigma_1) + S_2 - a_1 S_1)}{(S_2 + \Psi(1, \sigma_2) / (1 - a_2) \Psi(1, \sigma_2) + S_2 - a_2 S_1) - (S_2 + \Psi(1, \sigma_1) / (1 - a_1) \Psi(1, \sigma_1) + S_2 - a_1 S_1)} \end{aligned} \quad (8)$$

where $\Psi(r_D, \sigma_i)$ is defined as a similar kernel function.

(i) The outer boundary condition is infinite

$$\Psi(r_D, \sigma_i) = \frac{\Phi_{0,0}^i(r_D, R_D)}{\Phi_{1,0}^i(1, R_D)} = \frac{K_0(\sigma_i r_D)}{\sigma_i K_1(\sigma_i)}, \quad (9)$$

$$(R_D \rightarrow \infty) (i = 1, 2).$$

(ii) The outer boundary condition is closed

$$\Psi(r_D, \sigma_i) = \frac{\Phi_{0,1}^i(r_D, R_D)}{\Phi_{1,1}^i(1, R_D)} (i = 1, 2). \quad (10)$$

(iii) The outer boundary condition is a constant

$$\Psi(r_D, \sigma_i) = \frac{\Phi_{0,0}^i(r_D, R_D)}{\Phi_{1,0}^i(1, R_D)} (i = 1, 2). \quad (11)$$

Here, we get

$$\begin{aligned} a_i &= 1 + \frac{(1 - \omega)z - (1 - K)\sigma_i^2}{\lambda} (i = 1, 2), \\ \sigma_{1,2}^2 &= \frac{1}{2} \left\{ \left[\frac{\omega z + \lambda}{K} + \frac{(1 - \omega)z + \lambda}{1 - K} \right] \pm \sqrt{\left[\frac{(1 - \omega)z + \lambda}{1 - K} - \frac{\omega z + \lambda}{K} \right]^2 + \frac{4\lambda^2}{K(1 - K)}} \right\}. \end{aligned} \quad (12)$$

$\Phi_{i,k}^j(r_D, \xi)$ ($i = 1, 2; l, k = 0, 1$) are called as the functions of the guide solution, i.e.,

$$\Phi_{0,0}^i(r_D, \xi) = \varphi_{0,0}(r_D, \xi, \sigma_i),$$

$$\Phi_{1,0}^i(r_D, \xi) = \frac{\partial \Phi_{0,0}^i(r_D, \xi)}{\partial r_D} = -\sigma_i \varphi_{1,0}(r_D, \xi, \sigma_i),$$

$$\Phi_{0,1}^i(r_D, \xi) = \frac{\partial \Phi_{0,0}^i(r_D, \xi)}{\partial \xi} = \sigma_i \varphi_{0,1}(r_D, \xi, \sigma_i), \quad (13)$$

$$\Phi_{1,1}^i(r_D, \xi) = \frac{\partial^2 \Phi_{0,0}^i(r_D, \xi)}{\partial r_D \partial \xi} = -\sigma_i^2 \varphi_{1,1}(r_D, \xi, \sigma_i),$$

where $\varphi_{m,n}(x, y, \tau) = K_m(x\tau)I_n(y\tau) + (-1)^{m-n+1}I_m(x\tau)K_n(y\tau)$ and $K_\nu(\bullet), I_\nu(\bullet)$ are modified Bessel functions of the order ν . τ is a parameter.

Proof 1. Firstly, we prove the closed outer boundary condition.

The general solution to the government equation in the boundary value problem can be expressed as follows (the detailed derivation is given in Appendix A):

$$\begin{aligned} \bar{P}_{1D}(r_D, z) &= a_1 D_1 \frac{\varphi_{0,1}(r_D, R_D, \sigma_1)}{I_1(R_D \sigma_1)} \\ &+ a_2 D_2 \frac{\varphi_{0,1}(r_D, R_D, \sigma_2)}{I_1(R_D \sigma_2)}, \end{aligned}$$

$$\bar{P}_{2D}(r_D, z) = D_1 \frac{\varphi_{0,1}(r_D, R_D, \sigma_1)}{I_1(R_D \sigma_1)} + D_2 \frac{\varphi_{0,1}(r_D, R_D, \sigma_2)}{I_1(R_D \sigma_2)}, \quad (14)$$

where D_1, D_2 are arbitrary constants. Substitute $\bar{P}_{1D}(r_D, z)$ and $\bar{P}_{2D}(r_D, z)$ into Eq.(7) separately, the linear system about D_1, D_2 can be obtained as follows:

$$\begin{aligned} & \left[(1 - a_1) \frac{\varphi_{0,1}(1, R_D, \sigma_1)}{I_1(\sigma_1 R_D)} - (a_1 S_1 - S_2) \sigma_1 \frac{\varphi_{1,1}(1, R_D, \sigma_1)}{I_1(\sigma_1 R_D)} \right] D_1 \\ & + \left[(1 - a_2) \frac{\varphi_{0,1}(1, R_D, \sigma_2)}{I_1(\sigma_2 R_D)} - (a_2 S_1 - S_2) \sigma_2 \frac{\varphi_{1,1}(1, R_D, \sigma_2)}{I_1(\sigma_2 R_D)} \right] D_2 = 0, \\ & \left[C_D z \frac{\varphi_{0,1}(1, R_D, \sigma_1)}{I_1(\sigma_1 R_D)} + (K a_2 + 1 - K + C_D z S_2) \sigma_1 \frac{\varphi_{1,1}(1, R_D, \sigma_1)}{I_1(\sigma_1 R_D)} \right] D_1 \\ & + \left[C_D z \frac{\varphi_{0,1}(1, R_D, \sigma_2)}{I_1(\sigma_2 R_D)} + (K a_2 + 1 - K + C_D z S_2) \sigma_2 \frac{\varphi_{1,1}(1, R_D, \sigma_2)}{I_1(\sigma_2 R_D)} \right] D_2 = \frac{1}{z}. \end{aligned} \tag{15}$$

Because the boundary value problem has a unique solution, the determinant Δ of the coefficients of the linear system (namely, Eqs. (15)) about D_1, D_2 is not equal to zero. Now, according to the Cramer rule, the value of D_1, D_2 is obtained as follows:

$$\begin{aligned} D_1 &= -\frac{1}{z\Delta} I_1(\sigma_1 R_D) \left[(1 - a_2) \varphi_{0,1}(1, R_D, \sigma_2) \right. \\ & \quad \left. - (a_2 S_1 - S_2) \sigma_2 \varphi_{1,1}(1, R_D, \sigma_2) \right], \\ D_2 &= \frac{1}{z\Delta} I_1(\sigma_2 R_D) \left[(1 - a_1) \varphi_{0,1}(1, R_D, \sigma_1) \right. \\ & \quad \left. - (a_1 S_1 - S_2) \sigma_1 \varphi_{1,1}(1, R_D, \sigma_1) \right]. \end{aligned} \tag{16}$$

Where $\Delta =$

$$\begin{aligned} & \left[(1 - a_1) \varphi_{0,1}(1, R_D, \sigma_1) - (a_1 S_1 - S_2) \sigma_1 \varphi_{1,1}(1, R_D, \sigma_1) \right] \cdot \left[C_D z \varphi_{0,1}(1, R_D, \sigma_2) + (K a_2 + 1 - K + C_D S_2 z) \sigma_2 \varphi_{1,1}(1, R_D, \sigma_2) \right] \\ & - \left[(1 - a_2) \varphi_{0,1}(1, R_D, \sigma_2) - (a_2 S_1 - S_2) \sigma_2 \varphi_{1,1}(1, R_D, \sigma_2) \right] \cdot \left[C_D z \varphi_{0,1}(1, R_D, \sigma_1) + (K a_1 + 1 - K + C_D S_2 z) \sigma_1 \varphi_{1,1}(1, R_D, \sigma_1) \right]. \end{aligned} \tag{17}$$

Substituting Eq. (16) from Eq. (14), then we can obtain Eq. (8) by combining with Eqs. (9)–(11) and (12)–(13).

Similarly, when the outer boundary conditions are infinite and (7), the solution to boundary value problem can also be expressed as Eq.(8).

According to the boundary condition:

$$\left[\bar{P}_{2D} - S_2 r_D \frac{d\bar{P}_{2D}}{dr_D} \right]_{r_D=1} = \bar{P}_{wD}(z). \tag{18}$$

The dimensionless bottom hole pressure can be obtained

$$\begin{aligned} & \bar{P}_{wD}(z) \\ & = \frac{1}{z} \frac{1}{C_D z + (K a_2 + 1 - K / (1 - a_2) \Psi(1, \sigma_2) + S_2 - a_2 S_1) - (K a_1 + 1 - K / (1 - a_1) \Psi(1, \sigma_1) + S_2 - a_1 S_1) / (S_2 + \Psi(1, \sigma_2) / (1 - a_2) \Psi(1, \sigma_2) + S_2 - a_2 S_1) - (S_2 + \Psi(1, \sigma_1) / (1 - a_1) \Psi(1, \sigma_1) + S_2 - a_1 S_1)}. \end{aligned} \tag{19}$$

If let $S_1 = S_2 = S$, then Eq.(19) can be written as follows:

$$\bar{P}_{wD}(z) = \frac{1}{z} \frac{1}{C_D z + (a_2 - 1)(K a_1 + 1 - K) / (a_2 - a_1) [S + \Psi(1, \delta_1)] + (a_1 - 1)(K a_2 + 1 - K) / (a_2 - a_1) [S + \Psi(1, \delta_2)]}. \tag{20}$$

Now, we analyze the situation of $S_1 = S_2 = S$ as follows:

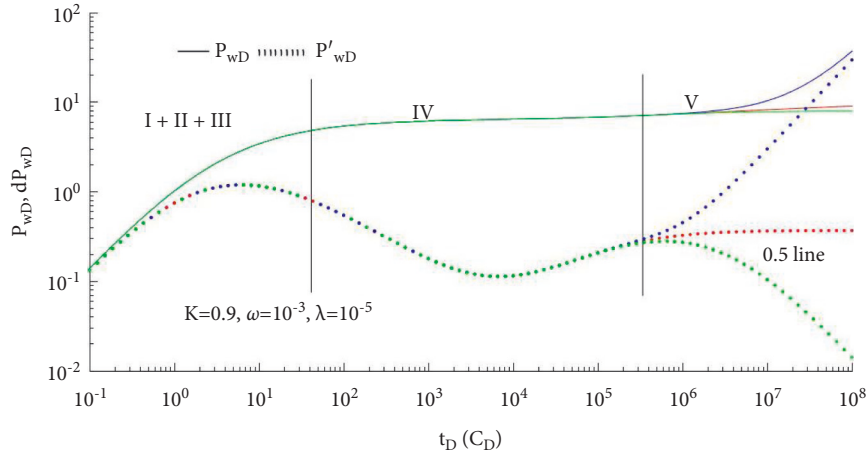


FIGURE 2: Special curves of the pressure and pressure derivative of dual permeability ($C_D e^{2S} = 1$, $K = 0.9$, $\omega = 10^{-3}$, $\lambda = 10^{-5}$).

$$\overline{P}_{wD}(z) = \frac{1}{z} \frac{1}{C_D z + 1 - K/S + \Psi(1, \sqrt{1 - \omega/1 - kz}) + K/S + \Psi(1, \sqrt{\omega/kz})}. \quad (21)$$

- (i) At the later time, when $t_D \rightarrow \infty$, $z \rightarrow 0$, then Eq. (20) can be written as follows:

$$\overline{P}_{wD} = \frac{1}{z} \frac{1}{C_D z + 1/S + \Psi(1, \sqrt{(1 - \omega/1 - k)z})}. \quad (22)$$

4. Chart Analysis

We draw the test well special curves of the dual permeability reservoir under three outer boundary conditions by using MATLAB software (Figure 2).

- (1) In Figure 2, the characteristic curves of both pressure and the pressure derivative are overlapping under three different outer boundary conditions in stages I-IV, which indicate that the changes in bottom hole pressure are the same before the pressure reaches the outer boundary.
- (2) Stages I-III are the early parts. Because of the influence of pure wellbore storage in the early times, the curves of the bottom hole pressure and pressure derivative coincide and show a line with a slope of 1. After the influence of pure wellbore storage, the curve of pressure derivative slopes downward after the peak appearance. The level of the peak value depends on the $C_D e^{2S}$.
- (3) Stage IV is the mid-party that mainly replies to the cross-flow characteristics of the transition zone, which are influenced by the mobility ratio K , storativity ratio ω , and cross-flow coefficient λ . We will conduct further analysis in part 4.2.
- (4) Stage V is the latter part that replies to the characteristics of radial flow in the dual permeability. When the outer boundary condition is closed, the pressure

derivative is a line with a slope of 1 (as shown by the blue dotted line in Figure 2). When the outer boundary condition is infinite, the pressure derivative is 0.5 line (as shown by the red dotted line in Figure 2), and when the outer boundary condition is a constant value, the pressure derivative will bend downwards (as shown by the green dotted line in Figure 2).

Now, we will analyze the impact of K, ω, λ on bottom hole pressure according to the chart (as shown in Figures 3-11). In Figures 3-5, we let $C_D e^{2S} = 1$, $\lambda = 10^{-5}$, $K = 0.9$ and let ω be equal to 10^{-1} , 10^{-2} , 10^{-3} , and 10^{-4} separately.

From Figures 3-5, we know that the changes of parameter ω have an obvious influence on the transition zone no matter how under which kind of outer boundary conditions. The stored energy ratio ω decides the width and depth of the concave pressure derivative curves in the transition section. With the decrease of a ω , the "concave" turns more deep and wide.

In Figures 6-8, we let $C_D e^{2S} = 1, \lambda = 10^{-5}, \omega = 10^{-3}$ and let K equal to 0.6, 0.9, 0.99, 0.999, respectively.

From Figures 6-8, we can obtain that the change of K has an obvious effect on the seepage zone of transition under the three different boundary conditions. For different values of K , the "concave" has different degrees of depth. The smaller the value of K , the "concave" is more shallower and approximately half of the value of the horizontal line. If $K = 5$, then we can get $k_1 h_1 = k_2 h_2$, and the characteristics of the curve are the same with the homogeneous reservoir model, the pressure derivative will not appear "concave", and the greater the value of K , the deeper the "concave".

In Figures 9-11, we let $C_D e^{2S} = 1, K = 0.9$, and $\omega = 10^{-3}$ and let λ be equal to 10^{-2} , 10^{-3} , 10^{-4} , and 10^{-5} , respectively.

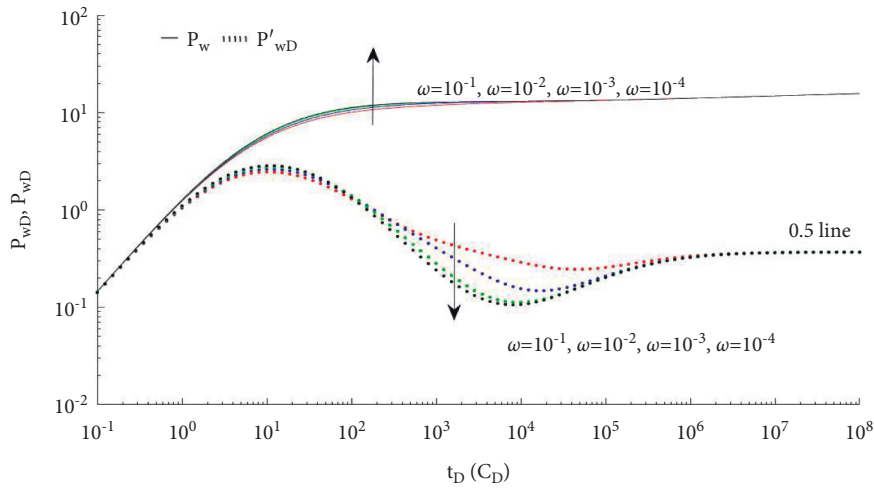


FIGURE 3: Dimensionless pressure of vertical wells under the infinite outer boundary influenced by ω ($C_D e^{2S} = 1, \lambda = 10^{-5}, K = 0.9$).

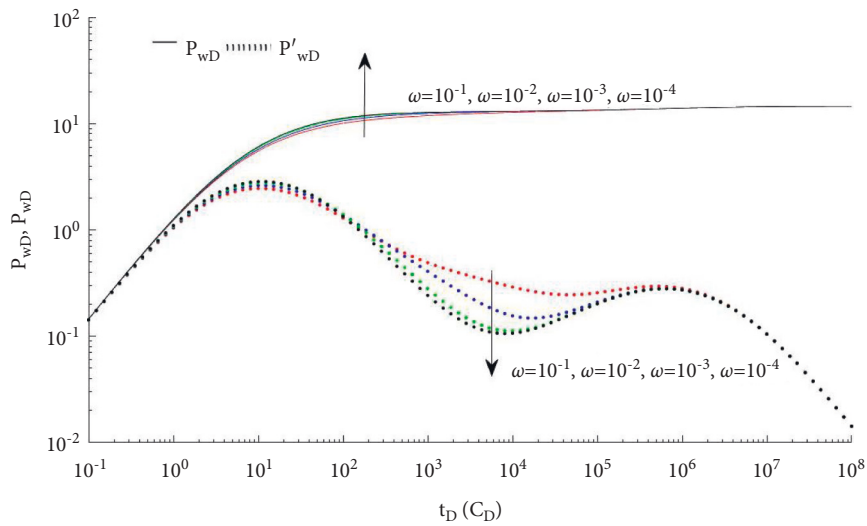


FIGURE 4: Dimensionless pressure of vertical wells under the constant outer boundary influenced by ω ($C_D e^{2S} = 1, \lambda = 10^{-5}, K = 0.9$).

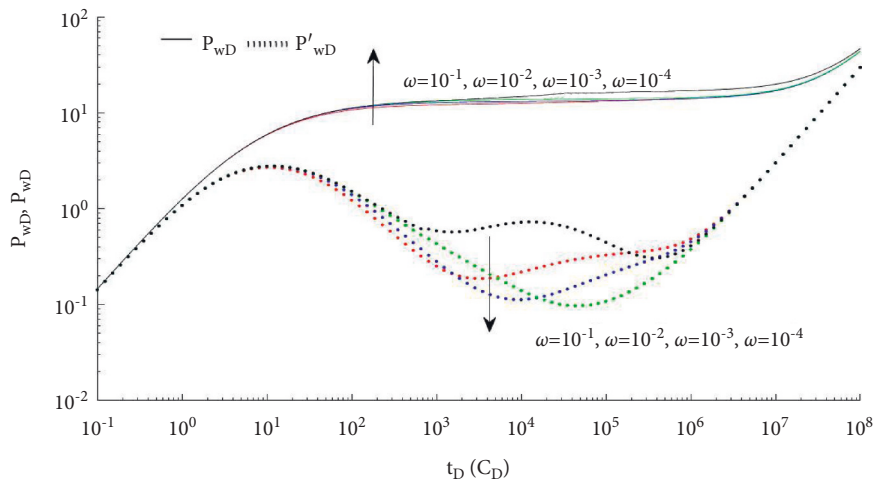


FIGURE 5: Dimensionless pressure of vertical wells under the close outer boundary influenced by ω ($C_D e^{2S} = 1, \lambda = 10^{-5}, K = 0.9$).

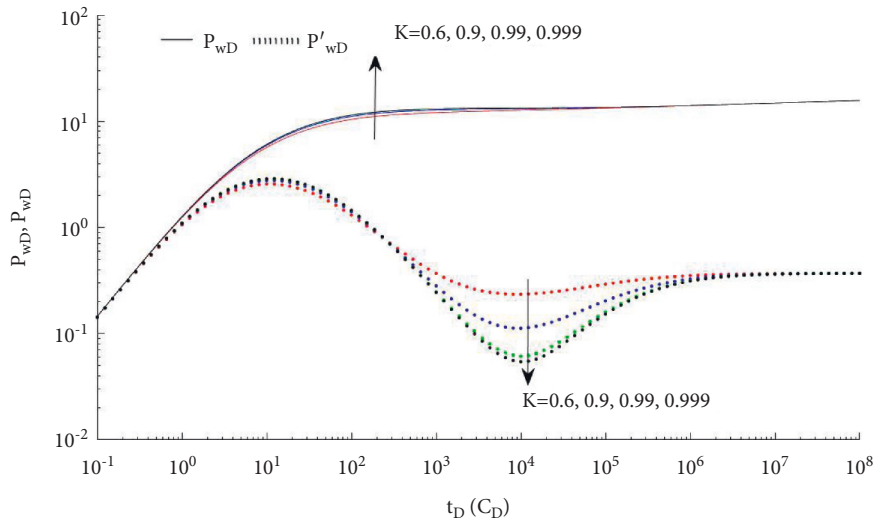


FIGURE 6: Dimensionless pressure of vertical wells under the infinite outer boundary influenced by K ($C_D e^{2S} = 1, \lambda = 10^{-5}, \omega = 10^{-3}$).

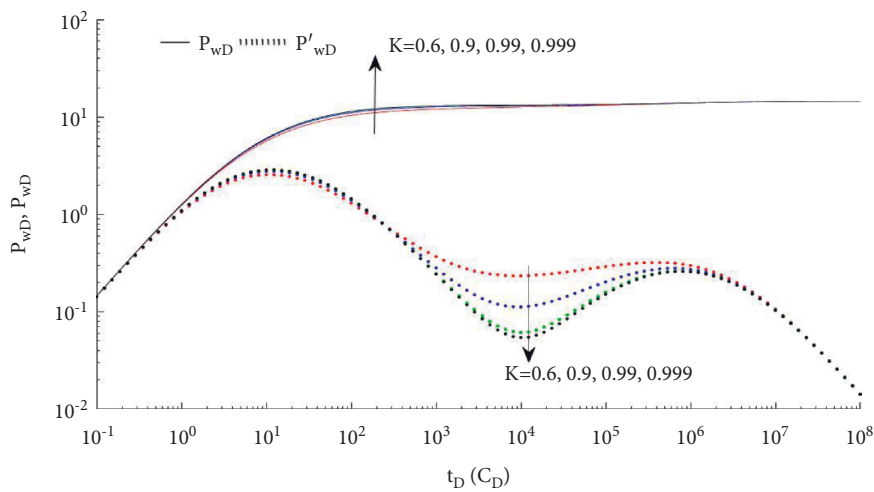


FIGURE 7: Dimensionless pressure of vertical wells under the close boundary influenced by K ($C_D e^{2S} = 1, \lambda = 10^{-5}, \omega = 10^{-3}$).

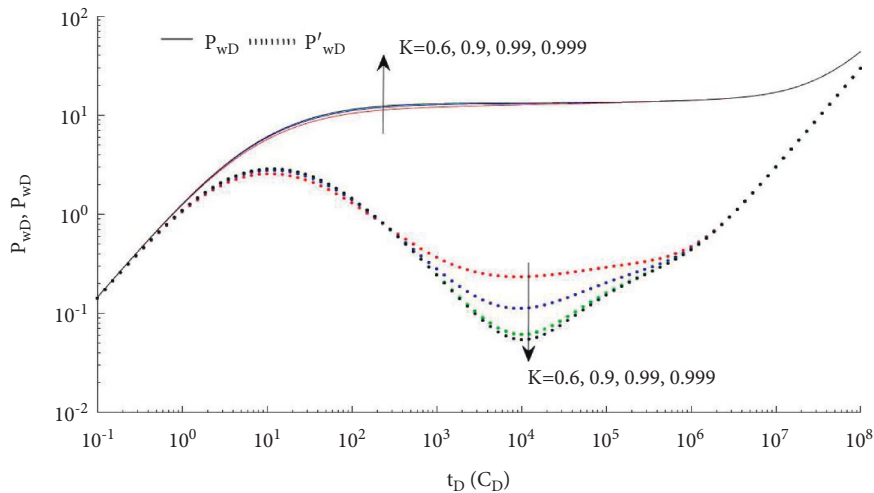


FIGURE 8: Dimensionless pressure of vertical wells under the constant boundary influenced by K ($C_D e^{2S} = 1, \lambda = 10^{-5}, \omega = 10^{-3}$).

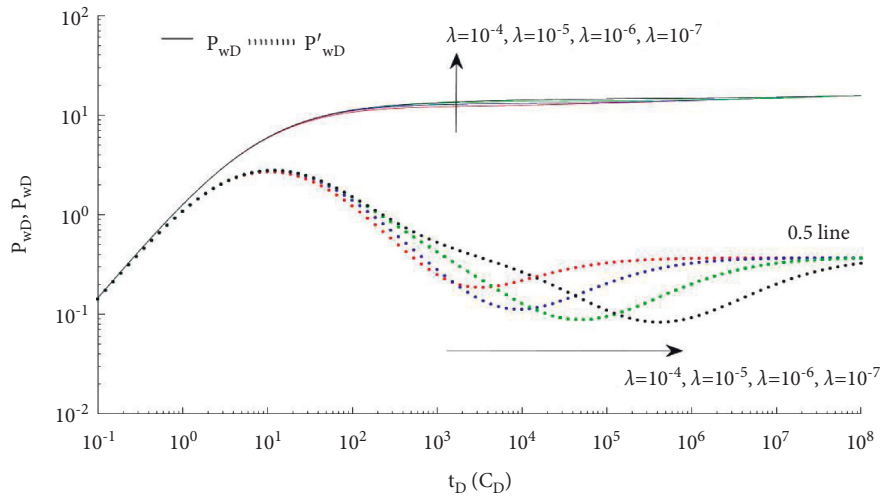


FIGURE 9: Dimensionless pressure of vertical wells under the infinite outer boundary influenced by λ ($C_D e^{2S} = 1, \omega = 10^{-3}, K = 0.9$).

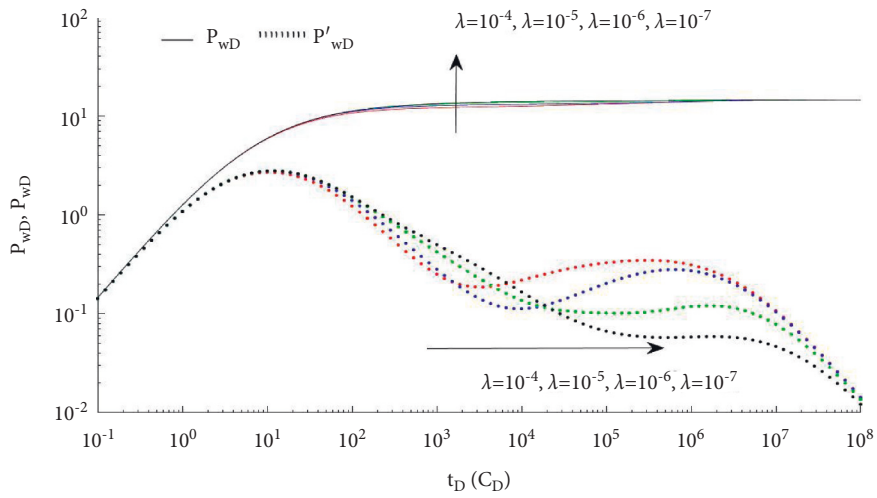


FIGURE 10: Dimensionless pressure of vertical wells under the constant value outer boundary influenced by λ ($C_D e^{2S} = 1, \omega = 10^{-3}, K = 0.9$).

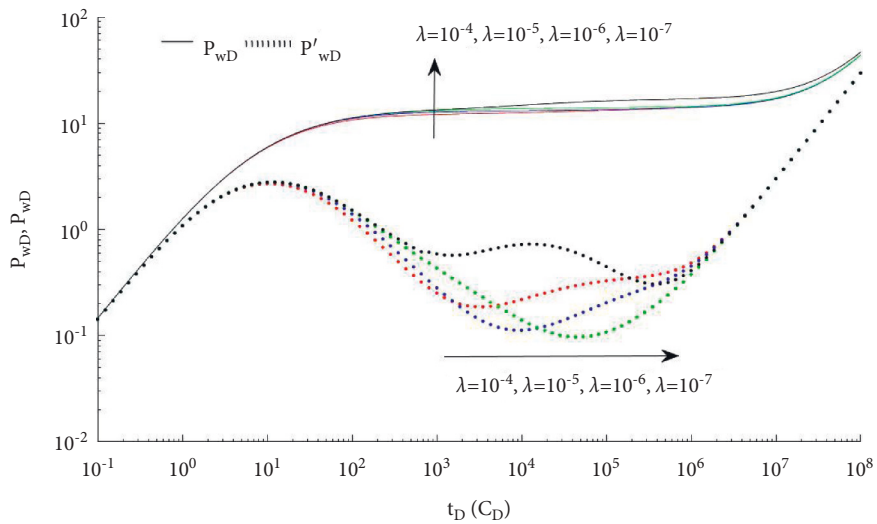


FIGURE 11: Dimensionless pressure of vertical wells under the close outer boundary influenced by λ ($C_D e^{2S} = 1, \omega = 10^{-3}, K = 0.9$).

From Figures 9–11, we can obtain that the position of the transition zone is determined by the cross-flow coefficient λ . The smaller value of λ , the later the transition zone appears, which reflects that the “concave” is on the right in Figures 9–11.

5. Conclusions

- (1) In this paper, we obtain the expression of bottom hole pressure of the dual permeability reservoir by using the SCM in Laplace space, and we provide a more complete testing chart for analyzing the change law of the pressure of dual permeability.
- (2) Using the SCM to solve the model of a vertical well in a dual permeability reservoir can avoid the cumbersome process of derivation, and the SCM only includes simple arithmetic, so it is easily understood and grasped. At the same time, the steps of SCM provide a clear algorithm flow for programs.
- (3) We obtain the simplified formula of solution (Eqs. (30) ~ (31)) for the model of the vertical well in a dual permeability reservoir, which contributes to analyzing the characteristics of the early and later parties in Figures 2–11.
- (4) We draw the curves of the bottom hole pressure and pressure derivative by using the modified Stehfest inversion formula and MATLAB software. We observe and analyze the change law of the curves by changing the mobility ratio K , storativity ratio ω , and cross-flow coefficient λ , which may provide an important theoretical value for further studying the dual permeability reservoir.

Appendix

In boundary value problem (7), the general solutions to governing system (7) can be expressed by modified Bessel functions $I_0(\sigma r_D)$, $K_0(\sigma r_D)$ as follows:

$$\begin{cases} \bar{P}_{1D}(r_D, z) = AI_0(\sigma r_D) + BK_0(\sigma r_D), \\ \bar{P}_{2D}(r_D, z) = CI_0(\sigma r_D) + DK_0(\sigma r_D), \end{cases} \quad (\text{A.1})$$

where A, B, C, D, σ are undetermined coefficients.

Substituting Eq.(A.1) into Eq (7), the system can be obtained as follows:

$$\begin{cases} AI_1(\sigma R_D) - BK_1(\sigma R_D) = 0, \\ CI_1(\sigma R_D) - DK_1(\sigma R_D) = 0, \end{cases} \quad (\text{A.2})$$

i.e.,

$$\frac{A}{B} = \frac{C}{D} = \frac{K_1(\sigma R_D)}{I_1(\sigma R_D)}. \quad (\text{A.3})$$

Substituting Eq.(A.3) into Eq.(A.1), respectively, the system can be obtained as follows:

$$\begin{cases} \bar{P}_{1D}(r_D, z) B \varphi_{0,1}(r_D, R_D, \sigma) / I_1(\sigma R_D), \\ \bar{P}_{2D}(r_D, z) D \varphi_{0,1}(r_D, R_D, \sigma) / I_1(\sigma R_D), \end{cases} \quad (\text{A.4})$$

where

$$\varphi_{m,n}(x, y, \tau) = K_m(x\tau)I_n(y\tau) + (-1)^{m-n+1}I_m(x\tau)K_n(y\tau).$$

By the property of the Bessel function [27], we know that $I_0(\sigma r_D)$, $K_0(\sigma r_D)$ satisfy the following equation:

$$Z_0''(x) = Z_0(x) + \frac{1}{x}Z_1(x). \quad (\text{A.5})$$

Substituting Eq. (A.4) into governing Eq. (7) and combining Eq.(A.5), the system can be obtained as follows:

$$\begin{cases} (K\sigma^2 - \omega z - \lambda)B + \lambda D = 0, \\ \lambda B + [(1-K)\sigma^2 - (1-\omega)z - \lambda]D = 0. \end{cases} \quad (\text{A.6})$$

According to Eq. (A.6), we obtain the equation as follows:

$$+ \frac{(\omega z + \lambda)[(1-\omega)z + \lambda] - \lambda^2}{K(1-K)} = 0. \quad (\text{A.7})$$

Solving the above equation, we obtain solutions as follows:

$$\begin{cases} \sigma_1^2 = \left\{ \frac{1}{2} \left[\frac{\omega z + \lambda}{K} + \frac{(1-\omega)z + \lambda}{1-K} \right] + \Delta \right\}, \\ \sigma_2^2 = \left\{ \frac{1}{2} \left[\frac{\omega z + \lambda}{K} + \frac{(1-\omega)z + \lambda}{1-K} \right] - \Delta \right\}, \end{cases} \quad (\text{A.8})$$

where

$$\Delta = \sqrt{\left[\frac{\omega z + \lambda}{K} - \frac{(1-\omega)z + \lambda}{1-K} \right]^2 + \frac{4\lambda^2}{K(1-K)}}. \quad (\text{A.9})$$

According to the structure principle of the solution to the homogeneous linear differential equation, we know that the linear combination of the two linear independent solutions is still the solution to the original equation. Therefore, solutions to governing system (7) can be expressed as follows:

$$\begin{aligned} & \bar{P}_{1D}(r_D, z) \\ & \bar{P}_{2D}(r_D, z) = D_1 \frac{\varphi_{0,1}(r_D, R_D, \sigma_1)}{I_1(R_D \sigma_1)} + D_2 \frac{\varphi_{0,1}(r_D, R_D, \sigma_2)}{I_1(R_D \sigma_2)}. \end{aligned} \quad (\text{A.10})$$

If Bof Eq. (A.6) recorded as aD , then we obtain

$$\begin{cases} (K\sigma^2 - \omega z - \lambda)aD + \lambda D = 0 \\ \lambda aD + [(1-K)\sigma^2 - (1-\omega)z - \lambda]D = 0. \end{cases} \quad (\text{A.11})$$

According to the above system, we can obtain

$$a = 1 + \frac{(1-\omega)z - (1-K)\sigma^2}{\lambda} \left(= -\frac{\lambda}{K\sigma^2 - \omega z - \lambda} \right). \quad (\text{A.12})$$

Hence, we obtain the following equation:

$$\begin{cases} a_1 = 1 + \frac{(1-\omega)z - (1-K)\sigma_1^2}{\lambda}, \\ a_2 = 1 + \frac{(1-\omega)z - (1-K)\sigma_2^2}{\lambda}. \end{cases} \quad (\text{A.13})$$

Data Availability

The data used to support the findings of this study are available from the corresponding author upon request.

Conflicts of Interest

The authors declare that they have no conflicts of interest regarding the publication of this article.

Acknowledgments

This work was supported by the Industry-University Research Innovation Funding of the Chinese University New Generation Information Technology Project (grant no. 2019ITA03033), 2021 Ministry of Education Collaborative Education Project (grant no. 202102588008), and the Guiding Project of the Scientific Research Plan of the Hubei Provincial Department of Education (grant no. B2021272).

References

- [1] R. S. Carvalho and A. J. Rosa, *Transient Pressure Behavior for Horizontal wells in Naturally Fractured Reservoir*, SPE 18302, Houston, Texas, USA, 1988.
- [2] K. A. Anil, A. M. Dawood, and M. Eddie, "Long-term field development opportunity assessment using horizontal wells in a thin, carbonate reservoir of the greater burgan field," *SPE Reservoir Evaluation and Engineering*, vol. 12, no. 1, pp. 14–24, 2009.
- [3] Z. D. Lei, S. Q. Cheng, X. F. Li, and H. P. Xiao, "A New method for prediction of productivity of fractured horizontal wells based on non-steady flow," *Journal of Hydrodynamics*, vol. 19, no. 4, pp. 494–500, 2007.
- [4] F. O. Jalal and T. Djebbar, "Transient pressure behavior of bingham non-Newtonian fluids for gorizontal well," *Journal of Petroleum Science and Engineering*, vol. 64, no. 1, pp. 21–32, 2008.
- [5] Y. F. He, X. G. Liu, and B. A. Xian, "Transient pressure analysis of gorizontal well for coalbed methane," *Coal Geology & Exploration*, vol. 35, no. 1, pp. 41–44, 2007.
- [6] R. H. Wang, R. C. Cheng, H. G. Wang, and Y. Bu, "Numerical simulation of transient cuttings transport with foam fluid in horizontal wellbore," *Journal of Hydrodynamics*, vol. 21, no. 4, pp. 437–444, 2009.
- [7] J. Hagoort, "A simplified analytical method for estimating the productivity of a horizontal well producing at constant rate or constant pressure," *Journal of Petroleum Science and Engineering*, vol. 64, no. 1-4, pp. 77–87, 2009.
- [8] W. J. Luo, Y. F. Zhou, and X. D. Wang, "A novel 3-D model for the water cresting in horizontal wells," *Journal of Hydrodynamics*, vol. 20, no. 6, pp. 749–755, 2008.
- [9] C. Q. Liu and X. D. Wang, "Transient anixisy-mmetrical two-dimensional flow through media with dual permeability," *Journal of Hydrodynamics*, vol. 6, no. 2, pp. 53–60, 1994.
- [10] J. C. Guo, R. S. Nie, and Y. L. Jia, "Dual permeability flow behavior for modeling horizontal well production in fractured-vuggy carbonate reservoirs," *Journal of Hydrology*, vol. 464-465, pp. 281–293, 2012.
- [11] D. Bourdet, *Pressure Behavior of Layered Reservoirs with Cross-Flow*, p. SPE13628, Bakerfield, California, USA, 1985.
- [12] J. Tian and D. K. Tong, "The flow analysis of fluids in fractal reservoir with the fractional derivative," *Journal of Hydrodynamics*, vol. 18, no. 3, pp. 287–293, 2006.
- [13] L. N. Hi and D. K. Tong, "Pressure analysis of dual permeability model in deformed medium with well bore storage effect," *Chinese Quarterly of Mechanics*, vol. 27, no. 2, pp. 206–211, 2006.
- [14] N. Q. Liu, *Interpretation of Modern Well Test Analysis*, Petroleum Industry Press, Beijing, 2008.
- [15] X. Y. Kong, *Hight Fluid Mechanics*, China Science and Technology Press, HeFei, 2010.
- [16] P. S. Zheng, S. C. Li, and Y. F. Zhang, "A class of quasilinear parameter boundary value problems for ordinary differential equations," *Journal of Northeast Normal University*, vol. 36, pp. 1–4, 2004.
- [17] J. Zou, X. Hu, Y. Y. Jiao et al., "Dynamic Mechanical Behaviors of Rock's Joints Quantified by Repeated Impact Loading Experiments with Digital Imagery," *Rock Mechanics and Rock Engineering*, 2022.
- [18] Z. C. Tang, Z. L. Wu, and J. Zou, "Appraisal of the number of asperity peaks, their radii and heights for three-dimensional rock fracture," *International Journal of Rock Mechanics and Mining Sciences*, vol. 153, Article ID 105080, 2022.
- [19] Y. Y. Jiao, K. Wu, J. Zou et al., "On the strong earthquakes induced by deep coal mining under thick strata-a case study," *Geomechanics and Geophysics for Geo-Energy and Geo-Resources*, vol. 7, no. 4, pp. 97–111, 2021.
- [20] P. L. Liu, S. C. Li, and L. Q. Zhao, "A general analysis of bottom-hole pressure distribution of dual permeability," *Oil and Gas Well Testing*, vol. 5, no. 5, pp. 9–11, 2004.
- [21] W. T. Sun, B. G. Huang, S. C. Li, and N. T. Wang, "Analysis of solving pressure of composite dual permeability reservoirs," *Journal of Southwest Petroleum College*, vol. 13, no. 5, pp. 90–95, 2006.
- [22] P. S. Zhen, S. C. Li, and W. C. Xu, "Method of well testing of dual permeability reservoirs base on similar structure of solution," *Journal of Southwest Petroleum College*, vol. 2, no. 30, pp. 108–110, 2008.
- [23] Q. Y. Li, S. C. Li, W. Li, and X. X. Xiao, "The problem of dual permeability reservoirs base on the similar structure," *Journal of Xi Hua University*, vol. 20, no. 2, pp. 64–66, 2011.

- [24] D. Wu, B. G. Huang, and S. C. Li, "The solving analysis of pressure of composite reservoirs," *Journal of Southwest Petroleum University*, vol. 29, no. 1, pp. 108–122, 2007.
- [25] X. W. Liao and P. P. Shen, *Model Well Test Analysis*, Petroleum Industry Press, Beijing, 2009.
- [26] J. Zou, W. Chen, D. Yang, H. Yu, and J. Yuan, "The impact of effective stress and gas slippage on coal permeability under cyclic loading," *Journal of Natural Gas Science and Engineering*, vol. 31, pp. 236–248, 2016.
- [27] S. S. Liu and S. D. Liu, *Special Function*, Meteorological Press, Beijing, 2002.